Fluorescence lidar for remote monitoring of plant

Kaifa Cao (曹开法)*, Bo Zhao (赵 博), Xin Fang (方 欣), Shaolin Wang (汪少林), Min Wang (王 敏), and Shunxing Hu (胡顺星)

Key Laboratory of Atmospheric Composition and Optical Radiation, Anhui Institute of Optics and Fine Mechanics, Chinese Academy of Sciences, Hefei 230031, China

**E-mail: caokaifa@tom.com*

Received May 11, 2009

The laser-induced fluorescence (LIF) characteristic of plant is directly linked to the photosynthesis. The LIF lidar for remote monitoring of plant has been suggested as one of the useful tools to identify plant species and determine its physiological status for a long time. So recently a LIF lidar for remote sensing of plant in Anhui Institute of Optics and Fine Mechanics is developed. It transmits laser beam at wavelength of 354.7 and 532 nm, and receives elastic echo and fluorescence echo at wavelength of 680 and 740 nm. Numerical simulations are carried out to determine achievable lidar performance including operation range. Validity of fluorescence signal is certified and then some results are presented. Comparison of the fluorescence characteristic among birch, conifer, and algae show that the fluorescence lidar is one of the potential tools to differentiate plant species.

OCIS codes: 010.3640, 120.0280, 300.2530.
doi: 10.3788/COL20100802.0130.

Climate change is a problem closely linked to human life. The concentration of atmospheric CO_2 increases every year because of the rapid development of global industry. It is very important to study sources and sinks of CO_2 in carbon circulation. The plant is one of the important sinks in the carbon circulation, at the same time it is the source of human activity and contributes to natural environment by its physiological action. Nowadays, many plants are being up against death and fading due to many complicated reasons such as the increment of pollution, water lack age, global warming, and so on. Understanding of vegetation state will give us a new access to unique earth conditions.

There are mainly three methods to be used as indicators for plant functioning, stress, and vitality: chemical method, hyperspectral remote sensing, and laser-induced fluorescence (LIF) lidar. Chemical method is not suitable for *in-vitro* intact measurement of living plants. Hyperspectral remote sensing[1] is based on plant spectral characteristics of reflectivity which is applied in large-scale monitoring. LIF emitted from chlorophyll is directly related to photosynthesis and has been used to detect the inner status of vegetation. Lidar[2,3] is an important tool to monitor atmospheric gases, atmospheric parameters, and objective characteristics. The LIF lidar[4−6] seems to be one of the most useful tools to remote diagnosis of vegetation status and distinguish different plant species.

The first LIF lidar was developed by Saito *et al.*[7] They tried to obtain the fluorescence echo from a sugar maple tree induced with a 337-nm nitrogen laser. Hoge *et al.* reported detection of LIF of green terrestrial plants by an airborne lidar[8]. In China, the first airborne ocean fluorescence lidar[9] was set up in Ocean University of China and the sea surface concentration of chlorophyll was deduced from fluorescence and Raman signal. The aiborne lidar can achieve large-scale measurement and has more availability. But aiborne lidars are more costly and technically complex. Usually, the groud lidar can be studied as the prototype to validate the feasibility of the system and offer essential data for researchers. In this letter, we introduce a LIF lidar system and then describe some results of LIF echo of natural living plants such as algae, conifer, and broadleaf.

Molecules in diversified matter have a series of electron energy states comprising vibrational and rotational states. In room-temperature condition, most molecules occupy the lowest electron energy state, which is called the ground state. Each of these energy states can be classified as singlet or triplet states, where the difference lies in the spin of the electrons. The molecules will be excited to a higher energy or excited state when they absorb radiation as far as the incident photon contains an energy equivalent to the difference between two allowed energy states. Due to instability of molecules in the excited state they will return to the ground state by relaxation process or deactivation process. But the relaxation process does not mean fluorescence emission, which is possible only if a once more relaxation happens after the electron transfers to the lowest energy level of the first excited state by other relaxation. Figure 1 displays six different transition or relaxation processes.

The equation of fluorescence lidar[4] can be expressed as

$$P_{\lambda_{\rm F}}(z) = P_{\lambda_0}\frac{1-A_{\lambda_0}}{4\pi}\frac{S}{R^2}\int\limits_{\Delta\lambda_{\rm F}}\eta(\lambda_{\rm F})\frac{\lambda_0}{\lambda_{\rm F}} \times T(z,\lambda_0)T(z,\lambda_{\rm F})\varphi_{\lambda_0\to\lambda_{\rm F}}{\rm d}\lambda, \quad (1)$$

where λ_0 and $\lambda_{\rm F}$ are wavelengths of output laser and fluorescence echo, respectively, $P_{\lambda_{\rm F}}$ is the echo signal of fluorescence channel, P_{λ_0} is the peak power of output laser, A is the reflection coefficient of object (also called as albedo), S is the area of the aperture of the receiving objective, R is the distance between lidar and the detected objective, φ is the quantum yield of fluorescence, T is single-pass atmospheric transmission between the lidar and the object such as plant, and η is the total lidar receive system efficiency at fluorescence wavelength

which includes reflectivity or transmission of optics and quantum efficiency of detector.

The Rayleigh-Mie lidar equation[10] as a function of range can be expressed as

$$P_{\mathrm{RM}}(R) = f_0(R)C_0P_0\frac{\beta_{\mathrm{a}}(R)+\beta_{\mathrm{m}}(R)}{R^2}\cdot \exp\left\{-2\int_0^z[\alpha_{\mathrm{a}}(\lambda_0,R')+\alpha_{\mathrm{m}}(\lambda_0,R')]\mathrm{d}R'\right\}, \quad (2)$$

where P_{RM} is the backscattered power as a function of range R, f_0 is geometric form factor, P_0 is the output power of the laser, C_0 is system constant , β_{a} and β_{m} are the backscattered coefficients of aerosol and molecular at wavelength λ_0, α_{a} and α_{m} are atmospheric extinction coefficients at wavelength λ_0.

The red LIF spectra of the chlorophyll of plant leaves are related with plant species and the status of vegetation. The intensity of the detected radiation is measured at three wavelengths: 685, 740, and 532 nm. The former two wavelengths are caused by the fluorescence of chlorophyll of a type a and b, respectively. The wavelength at 532 nm is needed for normalization of the detected LIF radiation. The intensity of chlorophyll fluorescence at 680 and 740 nm excited by 532 nm can be expressed as

$$P_{680} = P_{\lambda_0}\frac{\lambda_0}{680}\frac{1-A_{\lambda_0}}{4\pi}\frac{S}{R^2}\eta(680)T_{\lambda_0} T_{680}\varphi_{\lambda_0\to 680} \quad (3)$$

and

$$P_{740} = P_{\lambda_0}\frac{\lambda_0}{740}\frac{1-A_{\lambda_0}}{4\pi}\frac{S}{R^2}\eta(740)T_{\lambda_0} T_{740}\varphi_{\lambda_0\to 740}. \quad (4)$$

The ratio of the quantum yield of fluorescence at 740 nm to that at 680 nm is

$$R = \frac{\varphi_{\lambda_0\to 740}}{\varphi_{\lambda_0\to 680}} = \frac{740\cdot\eta(680)T_{680}P_{740}}{680\cdot\eta(740)T_{740}P_{680}}. \quad (5)$$

A mobile differential absorption lidar system[10,11] (AML-2) nowadays has been developed for day-night measurement of four kinds of pollutants such as SO_2, NO_2, O_3, and aerosol in lower troposphere. Recently, afluorescence detecting device was added for studying plant fluorescence characteristic. In the transmitter, laser beam with triple frequency of Nd:YAG at 354.7 nm is added, and two new filters, whose central wavelengths are 680 and 740 nm respectively, are loaded in the receiver. The schematic of the new lidar system is displayed in Fig. 2. It operates with the double and triple frequency of Nd:YAG (Brilliant B, 20 Hz) laser at 532 and 354.7 nm, whose pulse energies are accordingly about 50 and 200 mJ with repetition rate of 20 Hz and divergence less than 0.5 mrad. The laser beam is enlarged to reduce their divergence by a quintupling enlarger. After laser is transmitted in a direction of sounded objects by the transmitting mirror and scanning mirror, the backscattered light is accepted by a 30 cm-diameter Newtonian telescope. A field diaphragm and a fiber is displaced on the focus of the telescope. The radiation transmitted by the fiber is collimated by an ellipsoidal lens, then transits the filter group and attenuator group, and finally reaches photomultiplier tube (PMT). Then the electrical signal is directed to the input of the analog-to-digital converter (ADC) with a sampling frequency of 10 MHz. From the ADC, output digital data are saved in computer and wait for further analysis and process. Table 1 lists some specifications of this system. There are four filters fixed in ring flange of the filter group. Filters 1# and 2 # are used in receiving elastic lidar echo at wavelengths of 680 and 740 nm. Filters 3# and 4 # are used in receiving fluorescence lidar echo at wavelengths of 680 and 740 nm. Out-of-band blocking of filters 1# and 2 # is 1×10^{-4} from X-ray to FIR.

Table 1. Fluorescence Lidar Specification

Transmitter		
	Energy/Pulse	50 mJ (354.7 nm)
		200 mJ (532 nm)
	Repetition	20 Hz
	Beam Diameter	50 mm (∼0.2 mr divergence)
Telescope		
	Diameter	300 nm
	Focal Length	750 nm
Filter		
	Central Wavelength:	354.7 nm (#1) 532 nm (#2)
		680 nm (#3) 740 nm (#4)
	Full width at Half Maximum	1 nm (#1) 1 nm (#2)
		10 nm (#3) 10 nm (#4)
	Transmission:	50%(#1) 50% (#2)
		60%(#1) 60% (#2)

In order to predict the sensitivity of the lidar system, the performance of a LIF lidar has been simulated. The measurement sensitivity of the LIF lidar was analyzed in terms of the mean signal-to-noise ratio (SNR) of the lidar returns given by

$$\mathrm{SNR} = \frac{S\sqrt{T}}{\sqrt{S+2(N_{\mathrm{b}}+N_{\mathrm{d}})}}, \quad (6)$$

where S is the number of counts per time bin Δt for the signal acquisition resulted from lidar returned signal, N_{b} is the number of counts per time bin Δt resulted from the sky background, N_{d} is the number of counts per time bin Δt resulted from dark current, and T is the shot number of measurement. As can be seen from Eq. (1), to calculate the lidar returned signal S for the existed or proposed lidar instruments, it is only necessary to know the receiving and transmitting subsystems parameters and the optical parameters of a standard molecular atmosphere. Systems parameters are given in Table 1. The optical parameters of a standard molecular atmosphere were modeled by American Atmospheric Mode[10] as

$$\begin{cases} \alpha_{\mathrm{m}}(\lambda,Z) = 1.54\times10^{-3}\exp(-Z/7)(\frac{532}{\lambda})^4\times 8\pi/3 \\ \alpha_{\mathrm{a}}(\lambda,Z) = 2.47\times10^{-3}\exp(-Z/2)+5.1310^{-6} \\ \times\exp[-(Z-20)^2/36](\frac{532}{\lambda})\times S_1(\lambda), \end{cases} \quad (7)$$

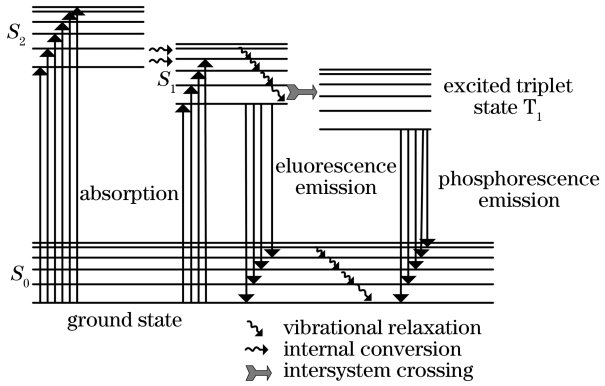

Fig. 1. The process of various energy transition of molecular interior as vibrational relaxation, internal conversion, external conversion, intersystem crossing, fluorescence emission, and phosphorescence emission.

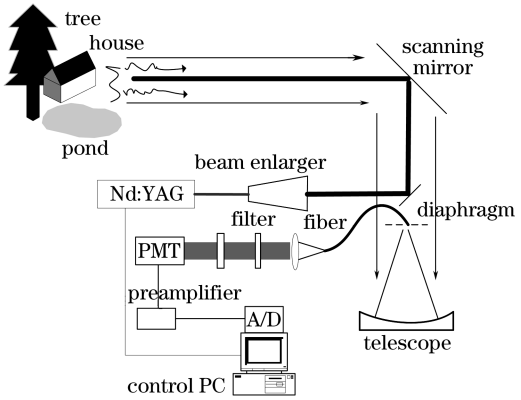

Fig. 2. Scheme of a new plant fluorescence lidar system based on AML-2 mobile lidar.

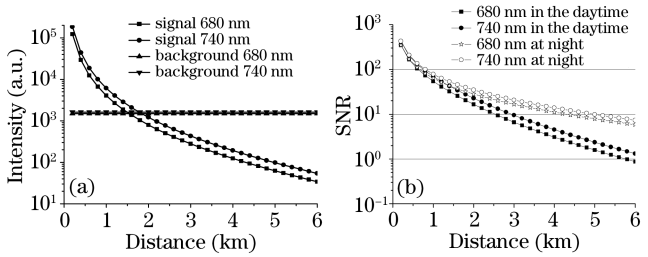

Fig. 3. The values of lidar signal, noise, and SNR.

where $\alpha_{\rm m}$ and $\alpha_{\rm a}$ is molecular and aerosol extinction coefficients, respectively, λ is wavelength, Z is altitude, S_1 is here chosen to be a constant value of 50 at wavelength of 532 nm as representative of tropospheric aerosol. The noise $N_{\rm b}$ was assumed as

$$N_{\rm b} = \eta P_{\rm b} \pi \left(\frac{\theta}{2}\right)^2 \Delta\lambda A_{\rm r}, \tag{8}$$

where $P_{\rm b}$ represents spectral radiance of the sky background, θ is the view of field of the lidar receiver, $\Delta\lambda$ is the bandwidth of filter, and $A_{\rm r}$ is the area of telescope. For most lidar systems, we can assume that the value of $N_{\rm d}$ is negligible and $N_{\rm b}$ in the night equals zero. So, according to Eqs. (1), (6), (7), and (8), lidar signal S, noise $N_{\rm b}$, and SNR (as illustrated in Fig. 3) are calculated. With the condition SNR = 1, we can conclude that the detected maximum range of lidar are about 2.5 km in the daytime and 4.2 km at night.

After the construction of fluorescence lidar was achieved, the validation of fluorescence would be necessary. Because the cross section of the fluorescence scattering is several orders of magnitude weaker than that of Mie-Rayleigh scattering, the lidar system must be capable of preventing the contamination of the fluorescence signal with spurious light from the elastic scattering. On 12.07.2007 between 20:00 and 21:10 Beijing Time, laser beam at wavelength 532 nm is transmitted to the surface of two kinds of materials (displayed in Fig. 3): leaves of broad-leaved plants and plastic of roof. When laser beam is transmitted to the plant, the elastic fluorescence scattering occurs simultaneously. So the elastic scattering is a sort of noise for fluorescence channel and must be suppressed. A filter is used in the fluorescence channel to suppress elastic light, so there is not echo signal of 532 nm (elastic light) at the distance between 250 and 300 m. The results in Fig. 3 testify the validation of fluorescence signals. The lidar echo results are shown in Fig. 4. It can be seen that there is fluorescence signal in lidar echo from plant, but not from wall. Therefore, the lidar system can receive the fluorescence signal correctly.

When the laser radiation reaches a definite level, nonlinear effects arise due to the saturation of the fluorescent response from the plant. The application of the pulsed radiation with Q-switch delay from 350 to 400 ns permits the analysis of the most intense, fast fluorescence (F) of nanosecond duration within the framework of the linear interaction of optical radiation with plant structures is illustrated by Fig. 5 which shows the dependence of the LIF signal on the laser intensity. As can be seen

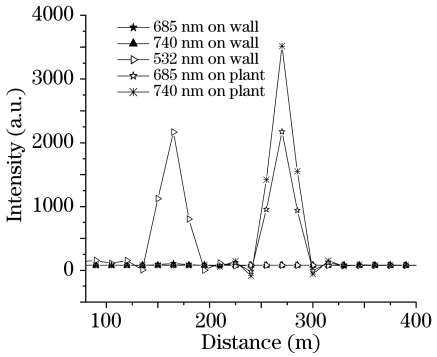

Fig. 4. Lidar signals from wall and plant.

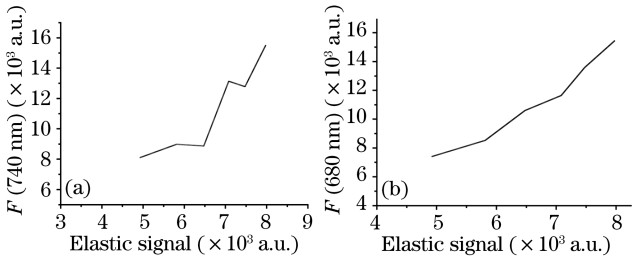

Fig. 5. The relationships between fluorescence signal and elastic signal.

Table 2. The Ratio (R) of the Fluorescence (F) at 740 nm to that at 680 nm with Different Plant

	Conifer	Broadleaf	Alage
F (680 nm)	1418.16	680.3	240.7
F (740 nm)	1607.47	533.66	5.93
R	2.3	1.7	0.054

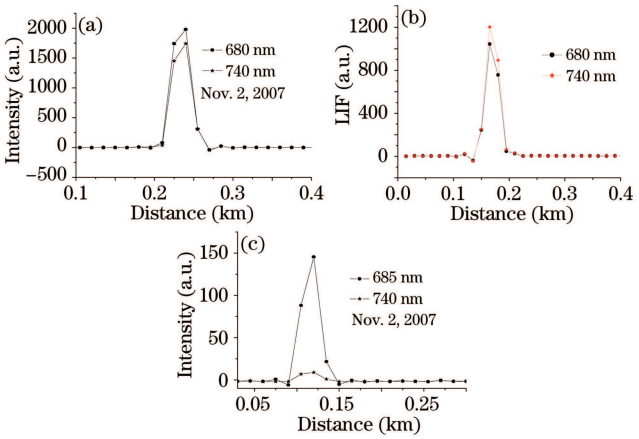

Fig. 6. Fluorescence signals emitted from (a) birth, (b) conifer, and (c) algae.

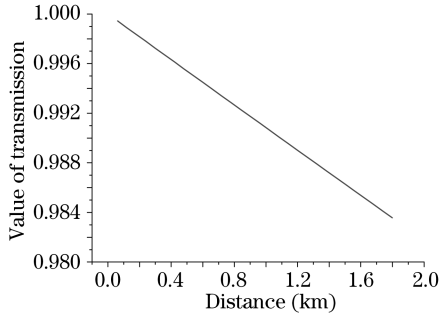

Fig. 7. Atmospheric transmission variation along with distance.

from the figure, there are no nonlinear effects, so our laser radiation have not reached the definite level.

To evaluate the feasibility of remote recognition of plant species, a series of experiments with broadleaf, conifer, and algae were conducted in field at Nov. 2, 2007. The laser at wavelength 532 nm is separately transmitted to broadleaf, conifer, and algae, at the same time the lidar echo is received and saved in computer. The fluorescence echo of broadleaf, conifer, and algae are shown in Figs. 6 (a)–(c). The algae differs from the other two plant types in that fluorescence at 740 nm is much weaker than that at 680 nm. Only the fluorescence of conifer at 740 nm is stronger than at 680 nm.

The ratio of the quantum yield of fluorescence at 740 nm to that at 680 nm is a significative value which relats the plant species to its status. In Eq. (5), the value of R can be retrieved from the lidar echo of fluorescence P, atmospheric transmission T at wavelength 680 and 740 nm, and the total lidar receive optical efficiency F. The lidar echo of fluorescence P is a value which can be measured in experiment. For short distances up to several hundred meters, we can assume the value of T(740 nm) /T(680 nm) to be 1, because the values of the transparency at 680 and 740 nm are very similar. The term of atmospheric transmission (displayed in Fig. 7, here we calculated atmospheric transmission using the standard atmospheric mode) within 1 km only makes a error less than 1% to the value of R. But when distance is very far or the atmospheric extinction coefficient is very large, we must calculate the values of the transparency at 680 and 740 nm from elastic lidar equation. For our lidar system, the transmission of filter and reflectivity of telescope at fluorescence wavelength is the same, so the lidar received optical efficiency is mainly determined by the sensitivity of PMT. We have F(740 nm) /F(680 nm)= 5, according to the characteristic of Hamamastu Tube R374 used in our mobile lidar system. Table 2 displays the values of ratio with broadleaf, conifer and algae which are calculated using the experimental fluorescence values.

In conclusion, a prototype lidar to study the plant fluorescence is established. The experimental result proves that the lidar echo is real fluorescence signal, and at the same time nonlinear effects of fluorescence echo does not arise in our lidar system. Our LIF lidar has possibility of remote diagnostics of plant species. The ratios of the fluorescence at 740 nm to that at 680 nm with different plants show that the system can be taken as an indicator of chlorophyll content and plant species.

This work was supported by the National High Technology Research and Development Program of China under Grant No. 2007FY110700.

References

1. J. Yang, J. Li, and D. Yang, World Geol. (in Chinese) **20,** 307 (2001).
2. P. Zhao, Y. Zhang, L. Wang, K. Cao, J. Su, S. Hu, and H. Hu, Chin. Opt. Lett. **6,** 157 (2008).
3. S. Wang, J. Xie, K. Cao, J. Su, P. Zhao, S. Hu, H. Wei, and H. Hu, Chinese J. Lasers (in Chinese) **35,** 739 (2008).
4. G. G. Matvienko, A. I. Grishin, O. V. Kharchenko, and O. R. Romanovskii, Opt. Eng. **45,** 056201 (2006).
5. F. E. Hoge, P. E. Lyon, C. W. Wright, R. N. Swift, and J. K. Yungel, Appl. Opt. **44,** 2857 (2005).
6. A. I. Grishin, O. V. Kharchenkoa, G. G. Matvienkoa, O. A. Romanovskiia, N. A. Vorobeva, and A. P. Zotikova, Proc. SPIE **4341,** 634 (2000).
7. Y. Saito, M. Kanoh, K. Hatake, T. D. Kawahara, and A. Nomura, Appl. Opt. **37,** 431 (1998).
8. F. E. Hoge, R. N. Swift, and J. K. Yungel, Appl. Opt. **22,** 2991 (1983).
9. W. Cheng, D. Wu, T. Zhang, and Z. Liu, Oceanologia ET Limnologia Sinica (in Chinese) **29,** 255 (1998).
10. K.-F. Cao, S.-L. Wang, Z.-Z. Wang, J. Xie, J. Su, P.-T. Zhao, and S.-X. Hu, Laser and Infrared (in Chinese) **38,** 429 (2008).
11. K. Qu, Y. Zhang, Z. Tao, X. Liu, G. Hong, Y. Zhao, and J. Su, Chinese J. Quantum Electron. (in Chinese) **23,** 365 (2007).